Journal of Biomedical Optics

SPIEDigitalLibrary.org/jbo

Application of the specular and diffuse reflection analysis for *in vitro* diagnostics of dental erosion: correlation with enamel softening, roughness, and calcium release

Ekaterina Rakhmatullina
Anke Bossen
Christoph Höschele
Xiaojie Wang
Barbara Beyeler
Christoph Meier
Adrian Lussi

SPIE

Downloaded From: http://biomedicaloptics.spiedigitallibrary.org/ on 01/14/2014 Terms of Use: http://spiedl.org/terms

Application of the specular and diffuse reflection analysis for *in vitro* diagnostics of dental erosion: correlation with enamel softening, roughness, and calcium release

Ekaterina Rakhmatullina,[a] Anke Bossen,[b] Christoph Höschele,[b] Xiaojie Wang,[a] Barbara Beyeler,[a] Christoph Meier,[b] and Adrian Lussi[a]
[a]University of Bern, Department of Preventive, Restorative and Paediatric Dentistry, Freiburgstrasse 7, Bern, CH-3010 Switzerland
[b]Bern University of Applied Sciences, OptoLab, Institute of Human Centered Engineering, Quellgasse 21, Biel, CH-2501 Switzerland

Abstract. We present assembly and application of an optical reflectometer for the analysis of dental erosion. The erosive procedure involved acid-induced softening and initial substance loss phases, which are considered to be difficult for visual diagnosis in a clinic. Change of the specular reflection signal showed the highest sensitivity for the detection of the early softening phase of erosion among tested methods. The exponential decrease of the specular reflection intensity with erosive duration was compared to the increase of enamel roughness. Surface roughness was measured by optical analysis, and the observed tendency was correlated with scanning electron microscopy images of eroded enamel. A high correlation between specular reflection intensity and measurement of enamel softening ($r^2 \geq -0.86$) as well as calcium release ($r^2 \geq -0.86$) was found during erosion progression. Measurement of diffuse reflection revealed higher tooth-to-tooth deviation in contrast to the analysis of specular reflection intensity and lower correlation with other applied methods ($r^2 = 0.42$–0.48). The proposed optical method allows simple and fast surface analysis and could be used for further optimization and construction of the first noncontact and cost-effective diagnostic tool for early erosion assessment *in vivo*. *© 2011 Society of Photo-Optical Instrumentation Engineers (SPIE).* [DOI: 10.1117/1.3631791]

Keywords: dental erosion; reflection analysis; diagnostics; enamel; roughness; hardness; calcium dissolution; scanning electron microscopy.

Paper 11258R received May 24, 2011; revised manuscript received Aug. 3, 2011; accepted for publication Aug. 8, 2011; published online Oct. 3, 2011.

1 Introduction

Caries remain among the most common diseases throughout the world and is associated with bacterial processes leading to damage of hard dental tissues (enamel, dentine, and cementum). Another growing problem in dental health is erosion, affecting up to 80% of adults and ~50% of children.[1] Dental erosion is defined as the loss of dental hard tissue by a chemical process without the impact of bacteria. Examples are enamel dissolution by acidic food beverages or due to gastric acid reflux and vomiting. The initial stage of dental erosion is characterized by softening of the enamel due to acidic demineralization and is a reversible process. Calcium ions derived from saliva flow may remineralize softened tissue and repair tooth mineral. However, if acidic impact persists, further dissolution of the enamel occurs, resulting in the partial layer-by-layer substance loss and decrease of the enamel thickness. This second stage of erosion is irreversible and might lead to the elimination of the enamel layer up to dentine in most severe cases (Fig. 1). This results in a painful experience and requires professional dental help.

To reduce erosive tooth wear, timely diagnostics and preventive strategies are of great importance. Although diagnostics of caries and preventive measures are well developed, clinical detection of dental erosion is based only on visual inspection. Particularly, observation of lesion characteristics on the facial/oral and occlusal/incisal surfaces, restorations rising above the level of the adjacent teeth, or shallow concavities on smooth surfaces indicate dental erosion.[2] The results of visual inspection are usually combined with the dietary, medical, and occupational features of the patient.[3] However, the estimation of the erosion progression might differ from dentist to dentist, depending on professional experience and education. Besides, the diagnosis of an early erosion stage is the most difficult but important step because preventive measures such as diet modification or application of dental products contribute to the significant decrease of the erosive tooth wear and, thus, a better quality of life for the patient.

Currently, various methods are proposed for the analysis of dental erosion,[4] but in spite of numerous advantages and disadvantages, the majority of them can be applied exclusively *in vitro* or *in situ*.[5] For instance, different "generations" of microradiography provide quantitative analysis of the dental tissue loss[6] but are not suited for *in vivo* erosion quantification due

Address all correspondence to: Ekaterina Rakhmatullina, University of Bern, Department of Preventive, Restorative and Paediatric Dentistry, Freiburgstrasse 7, Bern, Bern 3010 Switzerland; Tel: +0041316328603; Fax: +0041316328603; E-mail: ecatherin@yahoo.co.uk

1083-3668/2011/16(10)/107002/12/$25.00 © 2011 SPIE

Downloaded From: http://biomedicaloptics.spiedigitallibrary.org/ on 01/14/2014 Terms of Use: http://spiedl.org/terms

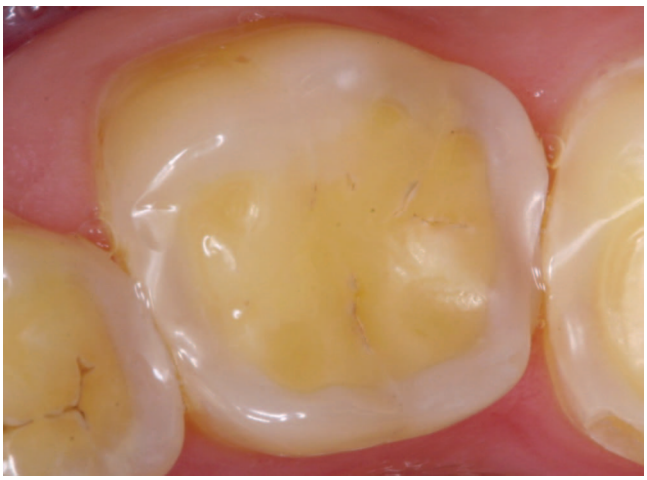

Fig. 1 Clinical example of dental erosion. The upper occlusal enamel tissue of the tooth is completely lost down to the remaining dentine layer (yellow color) that is exposed. The enamel (white surrounding ring) is only present on the sides of the tooth crown.

to long x-ray exposure times.[7] Quantitative light-induced fluorescence (LIF) allows detection of the early enamel demineralization based on the change of its autofluorescence signal.[8] Although this technique has a potential for *in vivo* application, the exact mechanism of the erosion detection is unclear. Optical coherence tomography (OCT) is another method that can be further developed for clinical quantification of erosion. Its measurement principle is described elsewhere.[9,10] Wilder-Smith et al.[11] reported *in situ* analysis of dental erosion by OCT in patients with gastroesophageal reflux disease, but the application of the technique was limited to enamel samples with severe substance loss of a few micrometers. Thus, it remains unclear if OCT can be applied for the analysis of early softening and initial substance loss. Many other measurement methods for the assessment of dental erosion induce mechanical or chemical damage of the dental tissues (profilometry,[12,13] permeability tests,[4,14] nanoindentations[15,16]), require time-consuming sample preparation procedures available under *in vitro* condition (scanning electron and atomic force microscopies[17–19]) or involve chemical analysis of the dissolved compounds (calcium, phosphorus).[20,21]

Among different optical methods, analysis of scattered and reflected light was mostly used for the diagnostics of caries. Light scattering analysis was applied for the *in vitro* quantification of carious lesions.[22,23] Attention was given to the change of reflectance spectra and reflectance intensity in the detection of carious enamel compare to a sound tissue.[24,25] Uzinov et al.[26] observed significant reduction of the specular reflection intensity by measuring the teeth with carious lesions using 450–900 nm wavelengths of light. Because caries development is also related to the acidic demineralization of the tooth, certain correlations can be expected between diagnostic criteria of caries and dental erosion. A first attempt to exploit reflection intensity for the investigation of dental erosion was published by Thomas et al.,[27] who used nitrogen LIF and diffuse reflection analysis to monitor erosion progression *in vitro*. Although a good correlation between LIF signal and erosion duration was reported, the increase of diffuse reflection with erosion time was not significant. Higher sensitivity of the LIF was concluded compare to the analysis of the diffuse light reflection.

This study attempted to: (*i*) validate application of both specular and diffuse reflection intensities for the *in vitro* diagnostics of early dental erosion, (*ii*) compare the optical measurement output to the standard analytical methods, and (*iii*) gather first information about the key parameters for further instrument optimization for *in vivo* erosion assessment. Application of the reflection analysis could allow construction of the noninvasive, cost-effective diagnostic tool providing a fast and quantitative output signal with no significant thermal or sound effect on the enamel surface and possibility to miniaturize the instrument for application in clinic. Here, the laboratory model of the reflectometer for enamel analysis was assembled with the goal of measuring signals of specular and diffuse reflected light in the wavelength range of 400–800 nm with a 45-deg angle of incidence and a variable angle of detection that was 45 deg for specular reflection and 0 deg for diffuse reflection analysis, respectively.

Quantification of the early erosion phases, i.e., softening of the enamel and initial substance loss, were targeted in this *in vitro* experiment as the most important stages for clinical diagnosis. Accordingly, erosive conditions were carefully adjusted. A series of test experiments were carried out before the main study in order to find out the optimal duration of the enamel incubation in acid inducing softening and primary substance loss only. Furthermore, citric acid with pH 3.6 was used as demineralizing agent to mimic a typical acidic environment in the oral cavity when commercial orange juice is consumed.[28] Hence, the obtained results from the reflection analysis of eroded enamel could be correlated with one or another stage of erosion progression that is clinically relevant knowledge for the assessment of tooth wear. To explain the observed tendencies, we monitored surface roughness of the enamel samples and visualized the treated dental surfaces by scanning electron microscopy. The analysis of enamel erosion by the proposed optical method was compared to the typically used analytical techniques in the field, such as measurement of the enamel hardness and calcium release from tooth surface into acidic solutions.

2 Experimental

2.1 *Materials*

2.1.1 *Chemicals*

Lanthanum nitrate hexahydrate [$La(NO_3)_3 \cdot 6H_2O$, Sigma-Aldrich Chemie GmbH, Steinheim, Germany), ≥99%] was used for the calcium analysis by atomic adsorption spectroscopy. Chloramin T trihydrate solution (≥98%, Sigma-Aldrich, Steinheim, Germany) was applied for the storage of extracted teeth as received. Citric acid (Merck, Stettlen, Switzerland, ≥99.5%) was used for the preparation of erosive solutions.

2.1.2 *Preparation of enamel specimens*

Caries-free human molars with no cracks on the buccal surfaces (microscopy examination, magnification ×20) were selected from a pool of extracted teeth. All teeth were extracted by dental practitioners in Switzerland (no water fluoridation, 250 ppm F^- in table salt) and were stored in 1% chloramin

Downloaded From: http://biomedicaloptics.spiedigitallibrary.org/ on 01/14/2014 Terms of Use: http://spiedl.org/terms

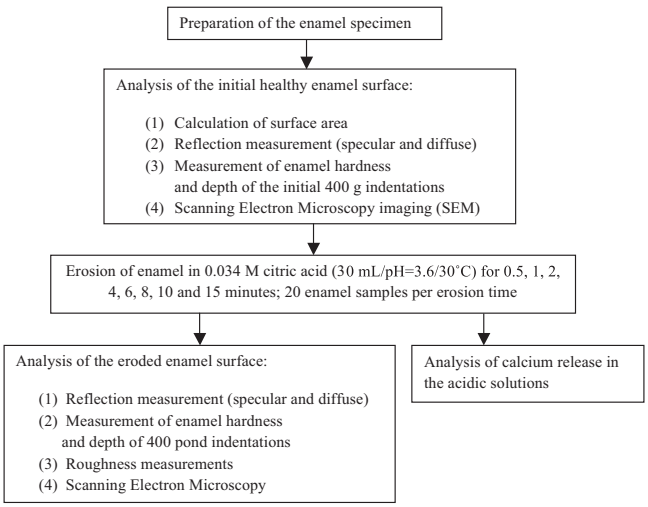

Fig. 2 Experimental design of the study.

T trihydrate solution. Before the extraction, the patients were informed about the use of their teeth for research purposes and consent was obtained. Teeth crowns were separated from the roots using an Isomet® Low Speed Saw (Buehler, Düsseldorf, Germany) and coated by red nail polish for the determination of the exposed enamel area (Sec. 2.2.1). The buccal sites of the specimens were embedded into the resin (Paladur, Heraeus Kulzer GmbH, Hanau, Germany) in two planar parallel molds. The thinner mold (200 μm thick) was removed while the teeth in the thicker one (7.5 mm thick) were serially abraded under constant tap-water cooling using a Knuth Rotor machine (LabPol 21, Struers, Copenhagen, Denmark) with silicon carbide paper disks of grain size 18.3 μm, 8 μm, and 5 μm, 60 s each. The embedded enamel blocks were taken out of the molds before being polished for 60 s with a 3-μm diamond abrasive on a Struers polishing cloth under constant cooling (LaboPol-6, DP-Mol Polishing, DP-Stick HQ, Struers, Copenhagen, Denmark). Between two polishing steps and after the final polishing, all slabs were sonicated for 1 min in tap water and rinsed. All prepared specimens had a flat ground enamel area with a 200-μm cutoff layer. Samples were stored in a mineral solution [1.5 mmol/l $CaCl_2$, 1.0 mmol/l KH_2PO_4, 50 mmol/l NaCl, pH 7.0 (Ref. 29)] and underwent further polishing with a 1-μm diamond abrasive (60 s, LaboPol-6, DP-Mol Polishing, DP-Stick HQ, Struers, Copenhagen, Denmark) immediately before the experiment.

2.1.3 *Erosion of enamel surface*

The prepared enamel specimens were immersed into 30 ml of citric acid (0.034 M, pH 3.6, similar to most of commercial orange juices) for 0.5, 1, 2, 4, 6, 8, 10, and 15 min (Fig. 2) under constant agitation (70 U/min, Salvis, Reussbühl, Switzerland) at 30°C. Samples were removed from acidic solutions, rinsed with deionised water (20 s), and dried with oil-free air (5 s). Twenty enamel specimens for each erosion time were used in the study; there were 160 specimens in total.

2.2 *Methods*

2.2.1 *Calculation of the exposed enamel surface area*

Every prepared enamel specimen was investigated under a light microscope (Leica M420) and the image of the exposed enamel was taken (Fig. 1, supporting information). Because of the red nail polish, the contour between the open (white) and resin-covered enamel (red) was well visible and could be clearly distinguished. The open enamel area was manually outlined (circled) using Software IM500, which further calculated the exposed surface taking into account the corresponding magnification factor of the microscope. Surface porosity was not included into the area calculation.

2.2.2 *Analysis of calcium loss in the acidic erosive solutions*

Acidic solutions were collected after the enamel erosion (Sec. 2.1.3) in order to analyze the amount of released calcium ions from every enamel specimen. Lanthan nitrate [$La(NO_3)_3 \cdot 6H_2O$, Merck, ≥99%] and 0.034 M citric acid (pH 3.6) were applied for the sample preparation. Analysis was carried out by means of a flame atomic adsorption spectrometer (AAnalyst 400, Perkin Elmer Analytical Instruments, Waltham, Massachusetts, USA) equipped with acetylene-air gas input. Lanthan nitrate (5%, aqueous solution) is used in the atomic adsorption analysis of calcium to hinder the interference of phosphate ions on the detection signal. The measured calcium concentrations were normalized to the corresponding enamel surface areas.

2.2.3 *Indentation measurement*

Microhardness analysis. Hardness measurements of the enamel specimen were performed using a Knoop diamond under a load of 50 g and a dwell time of 15 s (MHT-10 Microhardness Tester, Anton Paar, Paar Physica, Graz, Austria). Six indentations were made, with their long axis parallel to the vertical borders of the window, at 50-μm intervals. The length of each indentation was measured with an optical analysis system and transferred to a computer (Leica DMR Microscope, Leica Mikroskopie and Systeme GmbH, Wetzlar, Germany). The instrument was calibrated before each use. The enamel softening (S) was calculated in percentages as the ratio between the microhardness difference of initial and eroded enamel ($\Delta SMH = SMH_{t=0} - SMH_{t=x}$, where t erosion time, $x = 0.5$, 1, 2, 4, 6, 8, 10, and 15 min) to the initial microhardness value,

$$S = (\Delta SMH/SMH_{t=0})\ 100\%. \quad (1)$$

Control of enamel substance loss during erosion. All enamel samples were dried with compressed oil-free air. A defect-free area in the middle of the experimental area of the enamel specimen was selected where six indentations with a load of 400 gs were performed [Fig. 3(a)]. The length of indentations was measured using the optical system of microhardness tester before and after erosion of every enamel sample. Based on the length [L, 3(b)], the depth of impression [D, Fig. 3(b)] was calculated according to the equation $D = L/2 \cdot \tan\alpha$, where $\alpha = 3.75$ deg, a known parameter of the diamond indenter. The average from the measurement of six indentations on each tooth surface was taken for statistical data analysis.

Downloaded From: http://biomedicaloptics.spiedigitallibrary.org/ on 01/14/2014 Terms of Use: http://spiedl.org/terms

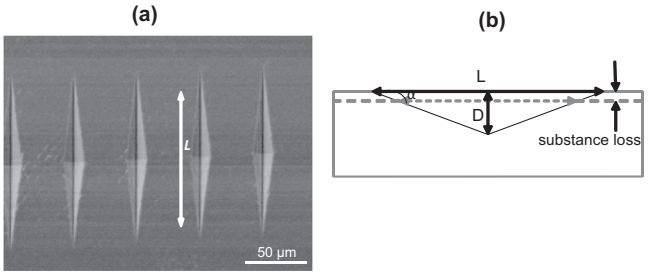

Fig. 3 (a) SEM image of the six indentations (400 g) on the healthy enamel surface. The length of indentations (L) was measured followed by (b) the calculation of the impression depth (D), which was used for the control of substance loss after erosive challenge.

2.2.4 *Scanning electron microscopy*

Representative specimens were mounted on aluminum stubs and sputtered with gold/palladium (100 s, 50 mA) using a sputtering device (Balzers SCD 050, Balzers, Liechtenstein). Scanning electron microscopy (SEM) was performed with a Stereoscan S360 scanning electron microscope at 20 kV (Cambridge Instruments, Cambridge, United Kingdom). Equal digital SEM micrographs (of 2000× and 5000× magnifications, respectively) were generated for each specimen (Digital Image Processing System, version 2.3.1.0, Point Electronic GmbH, Halle, Germany).

2.2.5 *Optical measurement of surface roughness*

For a noncontact roughness analysis, a high-resolution chromatic confocal point sensor (optical pen) was used (STIL sa, France, OP 300 VM). By moving the sample over a 1-mm distance using a motorized linear stage, 500 topography points were recorded at 300 Hz frequency. To calculate the roughness value, a linear fitting was performed to subtract the tilt effect of the sample followed by a polynomial fitting to remove the gross structure of the tooth. The roughness was defined as the standard deviation of the data after processing.

The roughness of 24 randomly chosen teeth with variable erosion times was measured before and after erosion (measurement 1). The measurement was then repeated on another spot in each tooth (measurement 2). The change of roughness was defined by R_e/R_o, where R_e is the roughness after erosion and R_o the original roughness of the noneroded enamel.

2.2.6 *Assembly of spectral resolved reflectometer*

The spectral resolved reflectometer consisted of a halogen source (Ocean Optics, Dunedin, Florida, USA, HL-2000-LVF-HP), an illumination arm and a measurement arm with varied angle position connected to a spectrometer (Ocean Optics, Dunedin, Florida, USA, USB-4000) (Fig. 4). The light source was coupled into a 600-μm fiber and focused on the sample through an optical system fixed at a 45-deg angle of incidence. The beam focus could be adjusted on the sample surface by moving the sample holder (height) up or down with a linear stage (Fig. 4). The illumination optic produced a spot size of 1.5-mm diameter. The measuring arm comprised 10× microscope objective (NA: 0.25) coupled to a 1000-μm fiber, thus limiting the measuring spot size to 1 mm. The position of the measurement arm could be switched between two angles of reflection: 0 and 45 deg to the surface normal. The 45-deg/0-deg (angle of incidence/angle of reflection) configuration was used for the measurement of diffuse reflection, while 45-deg/45-deg configuration was applied for the measurement of specular reflection. Reflection spectra at each configuration were recorded by the spectrometer and processed using the SpectraSuite software (Ocean Optics, Dunedin, Florida, USA).

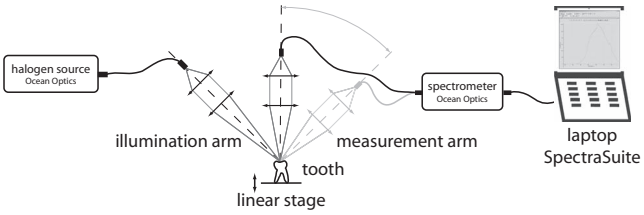

Fig. 4 Setup of the spectral resolved reflectometer.

2.2.7 *Measurements of diffuse and specular reflection from enamel surface*

The prepared enamel specimen was positioned on the sample holder so that the light spot was localized on the healthy enamel area without visible cracks. The SpectraSuite software was configured with a boxcar width (smoothing width) of 10 nm and a scan average of 2. First, the detector position was fixed at a 45-deg angle of reflection (Fig. 4) for the measurement of specular reflection spectrum. Because of natural tooth-to-tooth variability and slightly different sample heights after polishing procedures, the position of the sample holder and integration time were adjusted to obtain maximal reflection signal (i.e., 90% of the measuring range). The effect of the ambient light was subtracted by the elimination of the reflection spectrum recorded with the halogen light source being switched off. Afterward, the light was switched on and the reflection signal was recorded in the range of 400–800 nm. The measurement of specular reflection was performed for every sample before and after the erosive challenge.

For the analysis of diffuse reflection light, the position of the measurement arm was changed to a 0-deg angle of reflection (Fig. 4); however, sample position and height were kept constant during the entire procedure. Integration time was adjusted to achieve a reflection signal of ∼20% from a measurement range for healthy enamel surface before erosive treatment. The background reflection signal coming from the ambient light was subtracted analogous to the specular reflection experiment, and the diffuse spectrum was recorded in the range of 400–800 nm. The measurements of diffuse reflection were carried out before and after erosive treatments for every enamel sample. Integration time for the recording of specular or diffuse reflections was kept constant for every tooth sample during the entire experiment.

There were two specular (before and after erosion) and two diffuse (before and after erosion) reflection spectra recorded for every enamel sample. Both specular and diffuse spectral data were further processed according to the equation: R_r (%) $= [S(\text{eroded}) - S(\text{offset})/S(\text{noneroded}) - S(\text{offset})] \cdot 100$, where R_r is a relative calculated specular or diffuse reflection intensity from the enamel surface and S is the recorded signal from the enamel surfaces. R_r values were calculated in the whole wavelength region (400–800 nm). All reflection measurements

Downloaded From: http://biomedicaloptics.spiedigitallibrary.org/ on 01/14/2014 Terms of Use: http://spiedl.org/terms

were performed on dry enamel surfaces; the drying time was fixed to 6 min at room temperature in order to standardize the preparation conditions for all teeth.

2.3 *Experimental Design*

The erosive experiment was carried out with extracted human molar teeth applying different durations of enamel exposure to acid in order to vary the degree of erosive teeth demineralization. Twenty enamel samples for each of the eight different erosion times were used in the study; thus, there were 160 samples in total. Several different analytical techniques were included in the experimental design to correlate the results of optical reflection analysis with conventionally used microhardness and calcium dissolution measurements. To avoid the possible effect of microindentations on the measured reflection intensity from the enamel surface, the reflection analysis of the noneroded and eroded enamel samples was performed first, followed by the microhardness measurements (Fig. 2). Microhardness analysis of the initial noneroded enamel samples resulted in the presence of six indentations on the tested surface. These indentations could be occasionally included into the measurement spot during reflection analysis of the same enamel specimens after erosive treatment. To minimize the possibility of the interference between microindentations and the measured reflection intensity, no longitudinal erosive cycling model was applied in this study. Hence, every enamel sample was eroded only once for a defined time period and only six indentations were present on the surface during the second reflection analysis after erosive challenge. No indentations were made on the polished enamel surface before the first reflection analysis.

Additionally, enamel imaging and roughness examination were performed to explain observed changes of the reflection intensity during teeth erosion. The entire experimental design of the study is summarized in Fig. 2.

2.4 *Statistical Data Analysis*

Software R 2.9.11 was used for the descriptive statistical data analysis. Results are presented as box plots with marked outlier points (hollow circles). The correlation between analytical methods was calculated using Spearman rank coefficients (r^2) due to nonlinear functions.

3 Results

Analysis of the intensity of specular and diffuse reflection light was performed from the same enamel specimens before and after erosive treatment, prior to the microhardness measurements. The enamel incubation time in acid varied from 0.5 to 15 min to achieve softening and initial substance loss phases of erosion.

Figures 5(a) and 5(b) demonstrate, respectively, representative examples of specular and diffuse average spectra obtained from enamel surfaces eroded for 1, 2, 6, 8, and 15 min. The relative intensity of the specular and diffuse reflection was taken as 100% for the initial noneroded enamel samples. Obviously, intensity of the specular reflection decreased during erosion progression [Fig. 5(a)]. In contrast, intensity of the diffuse reflection increased with extended erosion time, especially at the initial erosive challenge [Fig. 5(b)]. We noted slightly higher sensitivity of the specular reflection signal for early erosion recognition at the wavelength region of 600–800 nm, whereas diffuse reflection had a more prominent signal change at 400–600 nm (Fig. 5). Because of the observed tendency, three wavelengths from different spectra parts were chosen for further data analysis (i.e., 400, 600, and 780 nm). The change of specular and diffuse reflection intensities over erosion time at three wavelengths is shown in Fig. 6. Fast decay of the specular reflection during initial acidic treatment of enamel [0.5–4 min, Fig. 6(a)] demonstrated its higher sensitivity toward analysis of early erosive stages compared to the diffuse reflection signal [Fig. 6(b)]. Furthermore, the standard deviations were larger in case of the diffuse reflection measurement. Medium correlation between specular and diffuse reflection signals was established (Table 1) at three chosen wavelengths. Spearman rank correlation coefficients were applied due to nonlinear functions.

Because reflection intensity is highly affected by the surface roughness,[30,31] special attention was given to the analysis of enamel roughness after erosive demineralization. Determination of enamel roughness by a confocal point sensor showed increase of roughness during erosion progression (Fig. 7). Measurements 1 and 2 correspond to the independent analysis of two different positions within the same enamel specimen. There

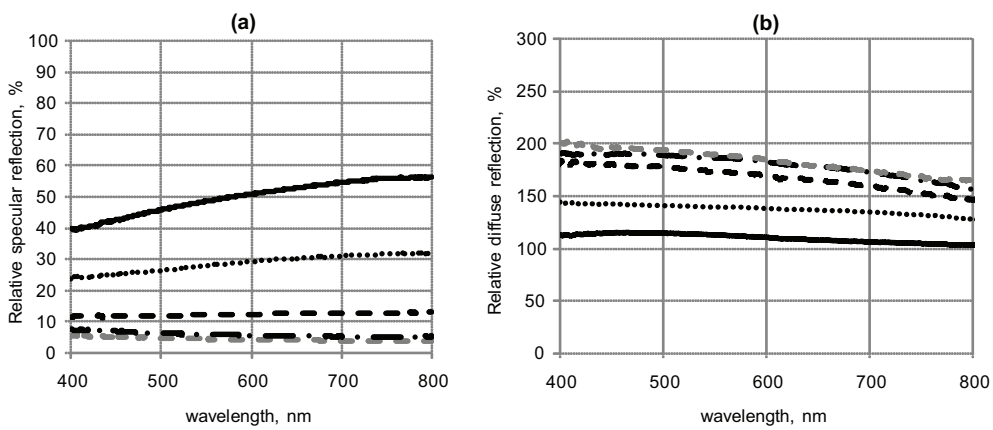

Fig. 5 Change of specular (a) and diffuse (b) reflection intensities during *in vitro* erosion of human enamel after 1 min (continuous line), 2 min (· · · · · ·), 6 min (▬ ▬), 8 min (▬ • ▬ •), and 15 min (▬ ▬).

Downloaded From: http://biomedicaloptics.spiedigitallibrary.org/ on 01/14/2014 Terms of Use: http://spiedl.org/terms

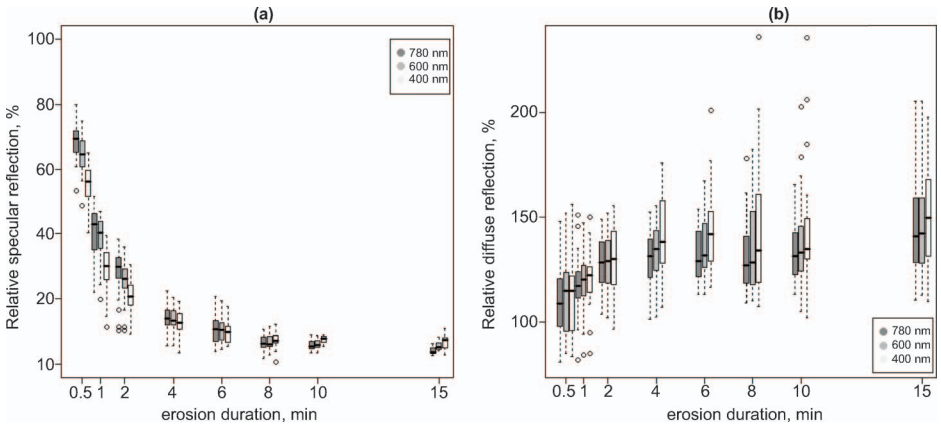

Fig. 6 Decrease of specular (a) and increase of diffuse (b) reflection intensities from enamel surfaces eroded for various time periods (0.5–15 min) *in vitro*.

were disparities of roughness values among enamel samples eroded for an identical time period. Inequality of the values can be related to the natural inhomogenity of dental tissues that, in turn, affects the measurements performed along the line on the surface and not from the specific surface area. Therefore, the presented roughness change (Fig. 7) should be interpreted as a tendency. Imaging of the enamel surface by SEM supported the results of optical roughness analysis. Figure 8 demonstrates examples of the enamel interface after incubation in acid for different time periods. Indeed, acidic etching of the enamel caused gradual rise of surface roughness and appearance of characteristic honeycomb erosive pattern.[32–34]

To characterize the degree of erosion progression, six indentations with a load of 400 gs were performed on every healthy enamel surface and their length was measured before and after acidic treatment. Large loads were used to leave a big trace on the surface [Fig. 3(a)] where the length of the impression could be quantitatively measured. When substance loss occurs (loss of enamel tissue) due to acidic dissolution, the depth of the original indentation decreases [Fig. 3(b)]. Figure 9 shows a depth change of the 400-g indentations as a function of the erosive duration. Apparently, no substance loss but softening was observed within first 2 min of acidic demineralization, as an average depth of impressions remained constant. Further incubation in acid led to a gradual decrease of the indentation depth, indicating initial enamel loss from the tooth surface. The indentation length could not be measured on the enamel samples eroded for >6 min due to severe etching and difficulty of recognizing the indentation lines.

Reduction of the specular and rise of the diffuse reflection signals, increased enamel roughness corroborated with the calcium release into acidic media [Fig. 10(a)]. Analysis of the calcium-ion release from dental tissues is one of the methods that is usually applied for *in vitro* erosion quantification. Calcium loss was measured by atomic adsorption spectroscopy and normalized to the surface area of the enamel specimen [Fig. 10(a)]. Dissolution of calcium ions typically results in the loss of enamel hardness.[35,36] Figure 10(b) illustrates gradual softening of the enamel upon incubation in citric acid (0.034M, pH 3.6). Indentations of a 50-g load were used for hardness analysis. Initially, linear progression of enamel softening with erosion time was followed by the decrease of softening rate after 8–10 min of demineralization. Nearly 8–10% of original hardness loss was detected already after 0.5 min of erosive impact.

High correlation coefficients ($r^2 \geq 0.8$–0.9) were found between change of specular reflection intensity (400, 600, and

Table 1 Spearman rank correlation coefficients (r^2) between the applied analytical methods. Negative correlation refers to the opposite tendencies of two measured parameters; for example, specular reflection intensity decreases, but diffuse reflection signal increases during erosion progression.

		Diffuse reflection	Calcium loss	Enamel hardness analysis
Specular reflection	400 nm	−0.463	−0.863	−0.86
	600 nm	−0.416	−0.915	−0.905
	780 nm	−0.49	−0.931	−0.924
Diffuse reflection	400 nm		0.463	0.465
	600 nm		0.427	0.426
	780 nm		0.479	0.478

Downloaded From: http://biomedicaloptics.spiedigitallibrary.org/ on 01/14/2014 Terms of Use: http://spiedl.org/terms

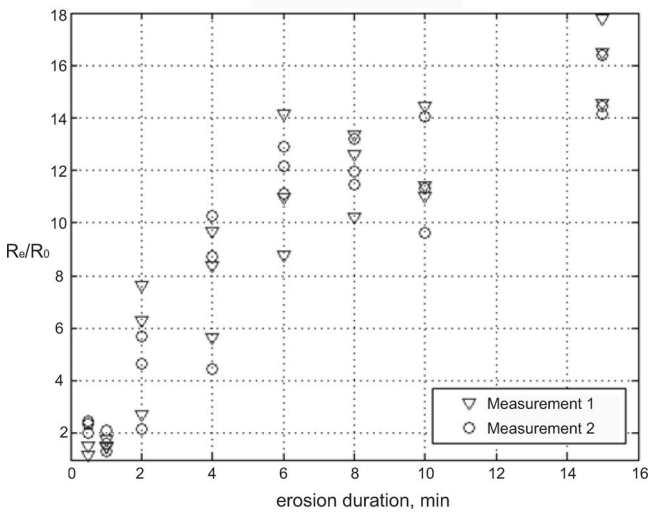

Fig. 7 Increase of the enamel surface roughness with erosion progression measured by confocal point sensor.

780 nm) and calcium release from the enamel surface as well as enamel hardness analysis (Table 1). These coefficient values were slightly higher in the case of measurements at 600 and 780 nm. However, only medium correlation was detected between the diffuse reflection signal and measurement of calcium loss and surface hardness (Table 1). This might be due to a lower sensitivity of the diffuse reflection intensity toward enamel etching and higher deviation of the measured signals compare to the specular reflection analysis. Note, the Spearman correlation coefficients were calculated taking into account all samples at all chosen erosion times, including outliers. The calculation of the statistical correlation coefficients at each particular erosion time was not performed due to a low sample number ($n = 20$ for each of erosion time).

4 Discussion

Examples of average spectra of specular [Fig. 5(a)] and diffuse [Fig. 5(b)] relative light reflections from enamel samples eroded for 1, 2, 6, 8, and 15 min are presented in a full measured wavelength range (i.e., 400–800 nm). The shape of the reflection spectra was in good agreement with the spectra of extracted human teeth measured by ten Bosch and Coops.[37] It is clearly visible, that the reflection change in both modes was most prominent on the early erosive stages (up to 2 min) while subsequent demineralization resulted in a less significant shift of the reflection intensity. To find an optimal wavelength for a maximal sensitivity of the current device, three wavelengths of 400, 600, and 780 nm were chosen from different spectra parts for data analysis and comparison. Relative intensity values of specular and diffuse reflection measured for eroded enamel samples were plotted as a function of erosion time for three chosen wavelengths (Fig. 6). Interestingly, the obtained results of the specular reflection signal [Fig. 6(a)] could be fitted by exponential function and showed a dramatic decrease of the reflection intensity during first 2 min of erosion. Thus, only 0.5 min of acidic treatment of the enamel led to 30–40% loss of surface

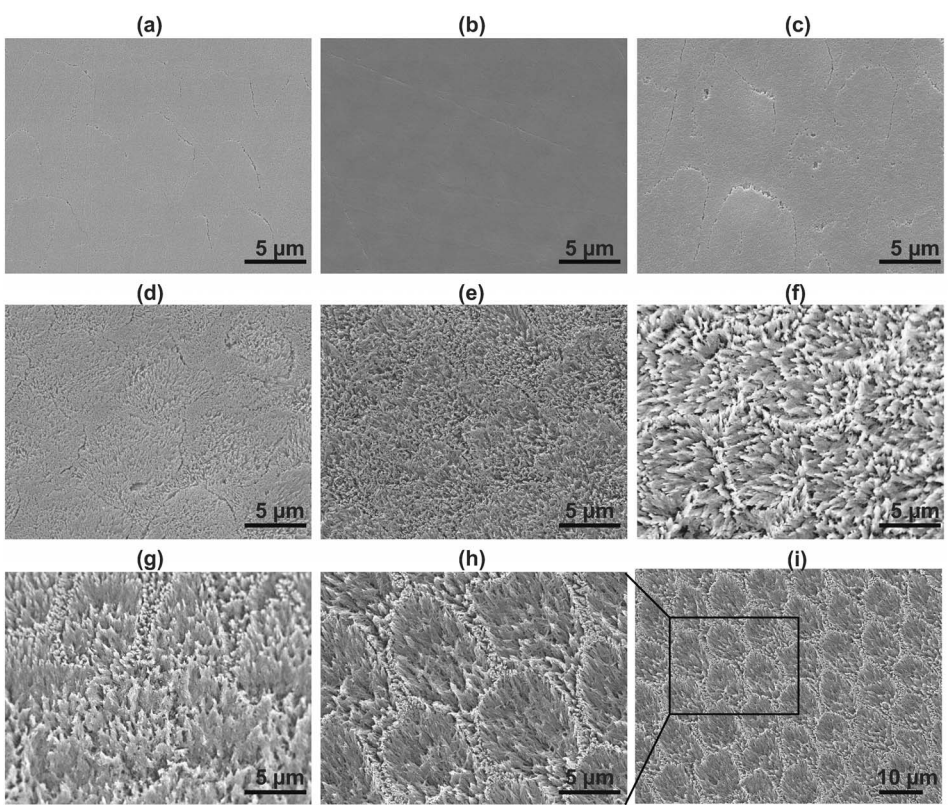

Fig. 8 Enamel surface after erosive treatment in citric acid for (a) 0.5, (b) 1, (c) 2, (d) 4, (e) 6, (f) 8, (g) 10, and (h) 15 min. (i) Last image (10-μm scale bar) shows typical honeycomb topography of the etched enamel surface, 15-min incubation in citric acid, pH 3.6.

Downloaded From: http://biomedicaloptics.spiedigitallibrary.org/ on 01/14/2014 Terms of Use: http://spiedl.org/terms

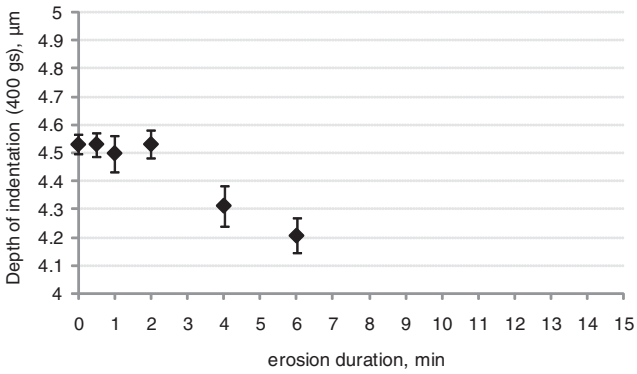

Fig. 9 Depth of 400-g indentations during incubation of enamel specimen in acid. The softening stage took place within first 2 min of erosion followed by initial substance loss.

reflectivity (100% corresponds to healthy enamel), followed by 60% decrease after 1 min of demineralization. The examples of the exponential curve fitting and assigned equations are presented in Fig. 2 (supporting information).

The data analysis showed no detectable difference between measurements at 400, 600, or 780 nm in case of a specular reflection signal [Fig. 6(a)]. All three curves showed exponential decay of the reflection intensity with similar deviations at each erosion time. The latter indicates that any of the three analyzed wavelengths can be applied for the analysis of specular reflection intensity from the tooth interface, and the results can be compared. It was noted that the deviation of the specular reflection values [Fig. 6(a), and Table 1, supporting information] was higher at the initial erosion stages and reduced once, approximately 6–8 min of acidic demineralization occurred. After 6–8 min of erosion time, the specular reflection intensity reached around 5–8% of its original value and seemed not to decrease further. In contrast to specular reflection analysis, measurement of diffuse reflection showed a 30–40% increase of the intensity from enamel surface after 2 min of erosive challenge, whereas subsequent incubation in acid did not cause significant change of the signal under the current setup configuration. Probably, the stabilization of the reflection intensity at the late erosive stages might be related to the measurement parameters of the reflectometer. We suggest that the signal sensitivity can be improved by optimizing the setup of the optical system. Moreover, signal deviation between enamel samples eroded for identical time was detected to be much higher in the case of diffuse reflection measurement than in the specular one (Fig. 6). As extracted human teeth were randomly chosen for the enamel preparation, this tendency can be partially explained by the impact of teeth natural color and inhomogeneity on the diffuse reflection signal.[37] Although tooth color is predominantly determined by the properties of the dentine, enamel can also contribute through the scattering at wavelengths at the blue range.[37] Remarkably, the deviations between enamel samples eroded for the same time duration were higher when the 400 nm wavelength was used for the measurements (Fig. 6). Detection of the diffuse reflection intensity at 600 and 780 nm did not lead to different results or deviation values and therefore can be considered to be identical. Standard deviation values (20 teeth for each erosion time) of the specular and diffuse reflection measurements are presented in Table 1 (supporting information).

For the method application, it was important to understand high sensitivity of the specular reflection analysis during the initial stages of acidic demineralization (first 6–8 min) and fast decay of the signal at longer demineralization times (≥8 min), i.e., exponential character of the fitted plot. It is well known that the light reflection depends on the surface roughness, wavelength, angle of incidence, and refractive index.[38,39] Because wavelengths (400, 600, and 780 nm) and angle of incidence were fixed in this study, the surface roughness and refractive index could be the main variables during acidic etching of the enamel. The enamel roughness was quantitatively measured by confocal point sensor, and the interface was additionally imaged by SEM. Figure 7 shows increase of the enamel surface roughness during erosion progression. Although the measurement results should be interpreted as a tendency, the continuous rise of the roughness in a nonlinear relation to the incubation time in acid was obvious. SEM images of the eroded enamel interface (Fig. 8) corroborated well the semiquantitative roughness analysis, showing slow etching of the surface and, thus, increase of its roughness. The etched pattern of the enamel appeared after

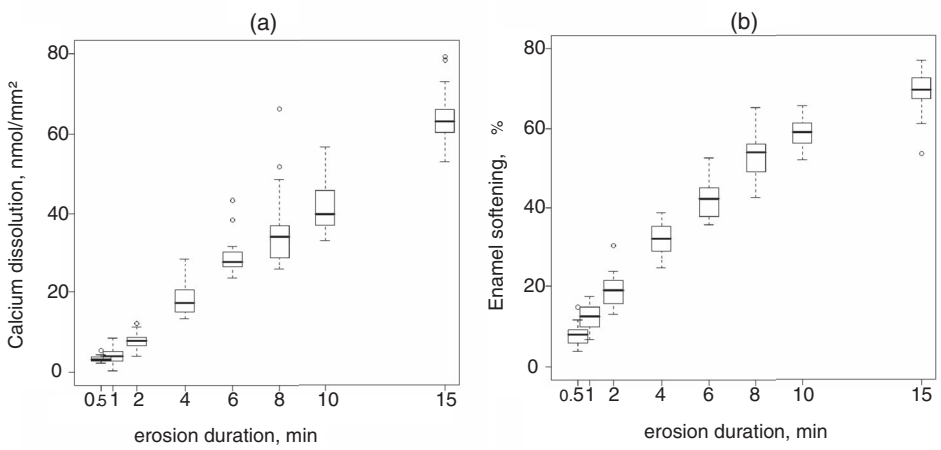

Fig. 10 (a) Calcium dissolution from enamel tissue into acidic probes after corresponding exposure time. (b) Enamel softening during acid-induced demineralization. Dashed lines in boxes represent mean values from measurements of 20 samples; empty circles are outlying data points.

Downloaded From: http://biomedicaloptics.spiedigitallibrary.org/ on 01/14/2014 Terms of Use: http://spiedl.org/terms

4 min of erosion [Fig. 8(e)] and became more prominent on the later erosive stages [Figs. 8(f)–8(i)]. Figure 8(i) demonstrates typical honeycomb topography of the eroded enamel.[32–34] At the same time, the surface of the enamel eroded for 8, 10, and 15 min looked rather similar, which correlated with the reduced rate of the roughness change after 8 min of erosion detected by confocal point sensor (Fig. 7). The observed increase of the enamel roughness could partially explain the exponential decay of the specular reflection intensity during erosion. Hence, after 6–8 min of acidic demineralization, increase of the enamel roughness slowed down; at the same time, specular reflection intensity reached minimal values and its decrease was less pronounced.

Also, the impact of the refractive index alteration on the specular reflection intensity cannot be excluded. It was shown that the enamel refractive index has a linear relation to the tissue density.[40] Acidic demineralization causes decrease of tissue density[41,42] and can potentially affect the refractive index of the enamel surface. Additionally, it was reported that the refractive index depends on the microroughness of the surface.[43,44] Elton[43] suggested that the increase of microroughness resulted in more air fraction relative to solid material, leading to a reduction in the effective refractive index. It might be applicable to the enamel surface as well because its porous structure changes architecture after acidic etching.[45] An increase of the pore volume[45] can contribute to the total air/solid ratio and, thus, to density and the effective refractive index of the enamel. In summary, both change of refractive index and surface roughness during enamel erosion could contribute to a great decrease of the specular reflection intensity within first seconds of demineralization. Taking into account a nearly 10 times increase of enamel roughness within the first 10 min of erosion, change of surface roughness can be considered as one of the main parameters determining specular reflection signal in the erosion analysis. To check the sensitivity of the proposed technique toward changes of enamel pore size, or density, demineralization/remineralization experiments could be performed. Although different remineralization procedures[46,47] might cause variation of the surface roughness in a broad range, application of mineral solutions containing calcium, phosphate, and fluoride ions mostly resulted in a nano-/microscale alteration of enamel tissue.[48] It was reported that the decrease of optical reflectivity from the remineralized enamel carious lesions was detected using polarization-sensitive optical coherence tomography (PS-OCT).[49]

The assignment of the reflection intensity to the particular erosion phase was one of the aims of the method development. The first phase of dental erosion is characterized by the enamel softening without loss of the mineral and is the most decisive stage for susceptibility of tissue toward subsequent abrasion.[50] However, no visible characteristic changes of the enamel appear on this phase making its visual diagnostics impossible. Further continuous demineralization can lead to the macroscopic loss of the enamel (Fig. 1). On the basis of these criteria, the phases of dental erosion can be assessed *in vitro* by the quantitative analysis of acid-induced substance loss. For the measurement of substance loss under the chosen experimental conditions, large 400-g indentations were performed on the healthy original polished enamel surface [Fig. 3(a)] and their depth was measured before and after erosive demineralization. It was proven that this method provides necessary sensitivity to detect small degrees of enamel wear by measurement of the indentation geometry.[51–53] Figure 9 presents at least two different phases of *in vitro* erosion. The first phase of dental erosion (i.e., softening of the enamel) took place within 2 min of the demineralization causing no substance loss and, thus, no change of the average indentations depth. Interestingly, it was the softening regime when the intensity of the specular reflection light had the fastest decrease (down to 20%) and diffuse reflection showed about a 30–40% increase of the intensity (Fig. 6). Depth of indentations started to decrease after 2 min of acidic incubation indicating the initial substance loss, second phase of the erosion (Fig. 9). A 6-min-long incubation resulted in the loss of ~300 nm of the enamel mineral (Fig. 9). After this phase, reflection change was no longer prominent, achieving nearly constant values. Hence, two phases of dental erosion could be well associated with a different change of the specular and diffuse reflection intensities. The depth of indentations was not measured at the later erosive times (≥6 min) due to significant roughness of the eroded enamel surface and difficulties of recognizing the indentation lines.

Softening and mineral loss of the enamel resulted in the release of calcium ions into acidic solution. The chemical mechanism of the acid-induced enamel dissolution is well explained by Featherstone and Lussi.[54] We measured calcium release by atomic adsorption spectrometry and compared the obtained results to the erosion assessment by reflection analysis. Softening of the enamel during first 2 min of demineralization caused ~10 nmol/mm^2 total calcium release accompanied by ~80% loss of the specular reflection intensity and a 30–40% increase of the diffuse reflection. The calcium loss rate did not depend on the softening or substance loss regime and showed linear function over erosion duration [Fig. 10(a)]. Hence, ~5 nmol/mm^2*min of calcium ions were dissolved into acidic media. Similar linear kinetics of enamel dissolution was reported earlier.[55,56] The analysis of the calcium content after short erosive treatment (0.5 min) required enamel samples with rather large surface areas to overcome the detection limit of the instrument. This was in contrast to the reflection analysis that allowed erosion detection after the first seconds of acidic challenge. However, measurement of calcium dissolution could be a more reliable method for the assessment of later stages of the erosion progression than reflection analysis, where little change of the reflection intensity occurred in the substance loss regime (Fig. 6). Apart from the analysis of calcium loss from the enamel surface, measurement of the enamel microhardness was applied as another typically used method for the *in vitro* erosion quantification. Incubation of the enamel samples in citric acid and calcium dissolution resulted in the gradual increase of the enamel softening [Fig. 10(b)]. After 2 min of acidic demineralization, ~20% softening of the enamel was detected. Subsequent hardness loss did not have linear relation to the enamel exposure time in acid. Unfortunately, direct comparison of the calcium release and enamel softening results to the data published by other authors was impossible due to variations of experimental conditions applied for *in vitro* erosion procedures.

The obtained values of enamel softening were used to find an equivalency of the applied erosive conditions to the clinically relevant situation. Note, the approximation should be considered with caution due to several reasons. First, the experiment design of the current *in vitro* study did not include a remineralization step after the erosive challenge; however, the remineralization

Downloaded From: http://biomedicaloptics.spiedigitallibrary.org/ on 01/14/2014 Terms of Use: http://spiedl.org/terms

process constantly occurs in the mouth due to salivary flow and the presence of an acquired pellicle layer on the enamel surface. Hannig et al.[57] showed that the pellicle layer provided certain protection of the enamel tissue from demineralization. Second, demineralization of enamel tissue by acidic drinks depends on drink pH, buffering capacity, type of acid (pKa), chelating and adhesive properties of the components, concentration of calcium and phosphate ions,[58–60] as well as the drinking method itself (holding the drink, long-sipping, gulping).[61] It was reported that 20-s-long drinking of 200 mL of orange juice (Rio d'oro, Aldi, Germany, pH 3.8) or Coke Light (Coca-Cola GmbH, Germany, pH 2.85) resulted in no detectable enamel softening (juice) or 15% softening (Coke), respectively.[57] The enamel specimens were incubated in the oral cavity for 2 h before the consumption of drinks.[57] In our *in vitro* study, 15% of enamel softening was achieved after 1 min of erosive treatment in citric acid [30 mL, pH 3.6, Fig. 10(b)]. For a rough approximation, 1 min of erosion applied in the study could be equivalent to a 20-s drink of 200 mL of Coke Light, both resulting in the same extend of enamel softening. Most probably, some remineralization of the softened enamel surface proceeds in the mouth just after the consumption of Coke, thus reducing the erosive effect. In conclusion, the erosive conditions applied in this *in vitro* study caused fast progression of dental erosion, which would require longer acidic impacts in the real-life situation to achieve similar enamel wear.

One of the important observations in this *in vitro* study was the high sensitivity of the reflection analysis toward the early erosion stage and its decay during further erosion progression. Thus, the diagnostics of dental erosion could still be possible by comparing the reflection signal from nonaffected and eroded dental tissues; however, the longitudinal monitoring over a long time period cannot be considered using the current setup of the instrument. In spite of the reduced sensitivity on late erosive stages, we believe that the proposed analytical technique has certain potential for intraoral application. Several parameters, such as the presence of an acquired salivary pellicle layer or plaque on the enamel surface, teeth abrasion, hydration degree, and native tooth color, should be considered for clinical measurements of the reflection intensity. It can be expected that the intensity of the specular reflection decreases in the presence of proteins (pellicle layer) or bacterial biofilm (plaque) on the enamel surface. We speculate that the reduction of the specular intensity by these soft layers could, most probably, depend on the layer thickness and density (i.e., parameters that usually differ from patient to patient as well as from tooth to tooth and cannot be clinically controlled). However, both pellicle layer and plaque can be partially removed from a particular dental surface for a diagnostic procedure; thus, their effect on the reflection intensity might be minimized. (De)hydration of the dental tissue during enamel preparation could be another parameter to consider in terms of clinical application of the reflectometer. It was shown that the dehydration degree of human enamel played an important role in measurements of light-induced fluorescence[62] or photothermal radiometry and modulated luminescence (PTR-LUM)[63] signals. Obviously, clinical study is required to evaluate the impact of the enamel preparation (removal of soft layers, drying) on the output signal of the optical instrument. We assume that these parameters must be standardized for clinical diagnostics.

Often abrasion contributes to the progression of dental erosion and complicates the erosion diagnostics. It is believed that abrasion (by tooth brushing, for example) contributes tremendously to the physical wear of softened etched enamel tissue, leading to a faster teeth decay.[64,65] It was shown in this study that the reflection intensity correlated with the change of surface roughness during continuous acidic etching. Abrasion causes removal of the softened enamel layer[65] and might potentially change the surface roughness and reflection intensity, accordingly. We suggest that abrasion via brushing the enamel surface can result in the decrease of the surface roughness of the etched softened enamel and, thus, an increase of the reflection intensity signal. A separate study about the effect of enamel abrasion on the specular reflection intensity was initiated, and the results will be published elsewhere.

The measurement of the relative reflection intensity (i.e., a ratio of intensities from eroded and noneroded enamel surfaces, in the same mouth) might minimize the effect of native tooth color and roughness on the reflection signal. The reference area can be found in the healthy dental area in a close proximity to the analyzed tooth surface.

5 Conclusion

The proposed optical device based on the analysis of reflection intensity can be successfully applied for the assessment of dental erosion of human enamel. Especially, specular reflection intensity can be recommended for the quantification of the early softening phase of dental erosion. The optical analysis of specular light reflection provided the best sensitivity among tested methods for the detection of enamel etching after first seconds of contact with the acidic environment. The decrease of the specular reflection intensity with erosion progression was mostly associated with the increase of surface roughness and could be fitted by exponential function. Measurement of the diffuse reflection revealed less sensitivity and a higher tooth-to-tooth deviation of signal.

The great advantage of the tested optical method is its simplicity, fast performance, noncontact, nondestructive analysis of dental tissue, and cost-effective assembly. The presented results can be further used for the optimization of measurement parameters and possible miniaturization of the reflectometer for *in vivo* dental application.

Acknowledgments

The authors thank Brigitte Megert and Dr. Tamara Koch for the scanning electron microscopy of the enamel samples, Stefanie Hayoz (Institute of Mathematical Statistics and Actuarial Sciences, University of Bern) for the statistical data analysis and Swiss Society of Odontology (Internal Project No. 253-10) for financial support of the research project.

References

1. T. Jaeggi and A. Lussi, "Prevalence, incidence and distribution of erosion," in *Dental Erosion from Diagnosis to Therapy*, A. Lussi, Ed., pp. 44–65, Karger AG, Basel (2006).
2. B. K. Gandara and E. L. Truelove, "Diagnosis and mangement of dental erosion," *J. Contemp. Dent. Practice* **1**(1), 1–17 (1999).

Downloaded From: http://biomedicaloptics.spiedigitallibrary.org/ on 01/14/2014 Terms of Use: http://spiedl.org/terms

3. C. Ganss, "How valid are current diagnostic criteria for dental erosion?," *Clin.Oral Invest.* **12**, 41–49 (2008).
4. T. Attin, "Methods for assessment of dental erosion" in *Dental Erosion from Diagnosis to Therapy*, A. Lussi, Ed., pp. 152–172, Karger AG, Basel (2006).
5. M. E. Barbour and J. S. Rees, "The laboratory assessment of enamel erosion: a review," *J. Dent.* **32**(8), 591–602 (2004).
6. J. Arends, J. L. Ruben, and D. Inaba, "Major topics in quantitative microradiography of enamel and dentin: R parameter, mineral distribution visualization, and hyper-remineralization," *Adv. Dent. Res.* **11**(4), 403–414 (1997).
7. C. Ganss, A. Lussi, and J. Klimek, "Comparison of calcium/phosphorus analysis, longitudinal microradiography and profilometry for the quantitative assessment of erosive demineralisation," *Caries Res.* **39**, 178–184 (2005).
8. M. H. van der Veen and E. de Josselin de Jong, "Application of quantitative light-induced fluorescence for assessing early caries lesions" in *Assessment of Oral Health. Monogr Oral Sci*., R. V. Faller, Ed., pp. 144–162, Karger AG, Basel (2000).
9. J. A. Izatt, K. Kobayashi, M. V. Sivak, J. K. Barton, and A. J. Welch, "Optical coherence tomography for biodiagnostics," *Opt. Photon. News* **8**(5), 41–47 (1997).
10. D. Huang, E. A. Swanson, C. P. Lin, J. S. Schuman, W. G. Stinson, W. Chang, M. R. Hee, T. Flotte, K. Gregory, C. A. Puliafito, "Optical coherence tomography," *Science* **254**(5035), 1178–1181 (1991).
11. C. H. Wilder-Smith, P. Wilder-Smith, H. Kawakami-Wong, J. Voronets, K. Osann, and A. Lussi, "Quantification of dental erosion in patients with GERD using optical coherence tomography before and after double-blind, randomized treatment with esomeprazole or placebo," *Am. J. Gastroenterol.* **104**, 2788–2795 (2009).
12. D. W. Bartlett, L. Blunt, and B. G. N. Smith, "Measurement of tooth wear in patients with palatal erosion," *Br. Dent. J.* **182**(5), 179–184 (1997).
13. E. Heurich, M. Beyer, K. D. Jandt, J. Reichert, V. Herold, M. Schnabelrauch, and B. W. Sigusch, "Quantification of dental erosion—a comparison of stilus profilometry and confocal laser scanning microscopy (CLSM)," *Dent. Mater.* **26**(4), 326–336 (2010).
14. A. Lussi, T. Jaeggi, and S. Schrärer, "The influence of different factors on *in vitro* enamel erosion," *Caries Res.* **27**(5), 387–393 (1993).
15. J. Arends and J. J. Ten Bosch, "Demineralization and remineralization evaluation techniques," *J. Dent. Res.* **71**(Spec. No.), 929–933 (1992).
16. T. Jaeggi and A. Lussi, "Toothbush abrasion of erosively altered enamel after intraoral exposure to saliva: an *in situ* study," *Caries Res.* **33**(6), 455–461 (1999).
17. J. H. Meurman and R. M. Frank, "Scanning electron microscopic study of the effect of salivary pellicle on enamel erosion," *Caries Res.* **25**(1), 1–6 (1991).
18. M. Finke, K. D. Jandt, and D. M. Parker, "The early stages of native enamel dissolution studied with atomic force microscopy," *J. Colloid. Interface. Sci.* **232**, 156–164 (2000).
19. S. Kasas, A. Berdal, and M. R. Celio, "Tooth structure studied using the atomic force microscope," *Proc. SPIE* **1855**(1), 17–25 (1993).
20. H. C. Margolis, Y. P. Zhang, C. Y. Lee, R. L. Kent,Jr., and E. C. Moreno, "Kinetics of enamle demineralization *in vitro*, "*J. Dent. Res.* **78**(7), 1326–1335 (1999).
21. R. P. Shellis, F. K. Wahab, and B. R. Heywood, "The hydroxyapatite ion activity product in acidic solutions equilibrated with human enamel at 37°C," *Caries. Res.* **27**(5), 365–372 (1993).
22. J. Brinkman, J. J. ten Bosch, and P. C. F. Borsboom, "Optical quantitation of natural caries in smooth surfaces of extracted teeth," *Caries Res.* **22**(5), 257–262 (1988).
23. J. J. ten Bosch, H. C. Van der Mei, and P. C. F. Borsboom, "Optical monitor of *in vitro* caries: a comparison with chemical and microradiographical determination of mineral loss in early lesions," *Caries Res.* **18**(6), 540–547 (1984).
24. C. L. Darling, G. D. Huynh, and D. Fried, "Light scattering properties of natural and artificially demineralised dental enamel at 1310 nm," *J. Biomed. Opt.* **11**(3), 034023 (2006).
25. M. Analoui, M. Ando, and G. K. Stookey, "Comparison of reflectance spectra of sound and carious enamel," *Proc. SPIE* **3910**, 227–234 (2000).
26. T. T. Uzinov, E. G. Borisove, K. P. Kamburova, and L. A. Avramov, "Reflectance spectroscopy of human teeth *in vitro*," presented at *BPU-5: 5th Conf. of the Balkan Physical Union*, Abstract No. SP16–003 (2003).
27. S. S. Thomas, R. J. Mallia, M. Jose, and N. Subhash, "Investigation of *in vitro* dental erosion by optical techniques," *Lasers Med. Sci.* **23**, 319–329 (2008).
28. D. Natanson, I. Gedalia, I. Reisstein, and A. Fuks, "Effect of fluoride pretreatment or rehardening with calcifying solutions on enamel softened by orange juice," *J. Dent. Res.* **52**(3), 625 (1973).
29. D. T. Zero, I. Rahbek, J. Fu, H. M. Proskin, and J. D. B. Featherstone, "Comparison of the iodide permeability test, the surface microhardness test, and mineral dissolution of bovine enamel following acid challenge," *Caries Res.* **24**(3), 181–188 (1990).
30. K.-E. Peiponen and T. Tsuboi, "Metal surface roughness and optical reflectance," *Opt. Laser Technol.* **22**(2), 127–130 (1990).
31. J. Liu, Y. Kazuo, Y. Zhou, and M. Sadayuki, "A reflective fiber optic sensor for surface roughness in-process measurement," *J. Manuf. Sci. Eng.* **124**(3), 515–522 (2001).
32. Z. J. Cheng, X. M. Wang, F. Z. Cui, J. Ge, and J. X. Yan, "The enamel softening and loss during early erosion studied by AFM, SEM and nanoindentation," *Biomed. Mater.* **4**, 015020 (2009).
33. T. Kodaka, M. Kuroiwa, and S. Higashi, "Structural and distribution patterns of surface "prismless" enamel in human permanent teeth," *Caries Res.* **25**(1), 7–20 (1991).
34. L. W. Ripa, A. J. Gwinnett, and M. G. Buonocore, "The "prismless" outer layer of deciduous and permanent enamel," *Arch. Oral Biol.* **11**(1), 41–48 (1966).
35. T. Attin, K. Meyer, E. Hellwig, W. Buchalla, and A. M. Lennon, "Effect of mineral supplements to citric acid on enamel erosion," *Arch. Oral Biol.* **48**(11), 753–759 (2003).
36. M. E. Barbour, D. M. Parker, and K. D. Jandt, "Enamel dissolution as a function of solution degree of saturation with respect to hydroxyapatite: a nanoindentation study," *J. Colloid. Interfac. Sci.* **265**(1), 9–14 (2003).
37. J. J. ten Bosch and J. C. Coops, "Tooth color and reflectance as related to light scattering and enamel hardness," *J. Dent. Res.* **74**(1), 374–380 (1995).
38. D. L. Jaggard and X. Sun, "Fractal surface scattering: a generalized Rayleigh solution," *J. Appl. Phys.* **68**(11), 5456–5462 (1990).
39. X. D. He, K. E. Torrance, F. X. Sillion, and D. P. Greenberg, "A comprehensive physical model for light reflection," *Comp. Graphics* **25**(4), 175–183 (1991).
40. R. S. Manly, "Relation of refractive index to density in dental hard tissues," *J. Am. Chem. Soc.* **60**(12), 2884–2886 (1938).
41. A. Boyde, "Dependence of rate of physical erosion on orientation and density in mineralised tissues," *Anat. Embryol.* **170**(1), 57–62 (1984).
42. B. D. Schmuck and C. M. Carey, "Improved contact x-ray microradiographic method to measure mineral density of hard dental tissues," *J. Res. Natl. Inst. Stand. Technol.* **115**(2), 75–83 (2010).
43. N. J. Elton, "Surface finish and microroughness of filled nylon injection mouldings," *Reflectometry application note* **7**, pp. 1–6, www.surfoptic.com.
44. I. Ohlidal and F. Lukes, "Ellipsometric parameters of randomly rough surfaces," *Opt. Commun.* **5**, 323–326 (1972).
45. T. T. Nguyen, A. Miller, and M. F. Orellana, "Characterization of the porosity of human dental enamel and shear bond strength *in vitro* after variable etch times: initial findings using the BET method," *Angle Orthod.* **81**(4), 707–715 (2011).
46. J. Mathias, S. Kavitha, and S. Mahalaxmi, "A comparison of surface roughness after micro abrasion of enamel with and without using CPP-ACP: an *in vitro* study," *J. Conserv. Dent.* **12**(1), 22–25 (2009).
47. Z. Dong, J. Chang, Y. Zhou, and K. Lin, "*In vitro* remineralization of human dental enamel by bioactive glasses," *J. Mater. Sci.* **46**, 1591–1596 (2011).
48. N. J. Cochrane, F. Cai, N. L. Hug, M. F. Burrow, and E. C. Reynolds, "New approaches to enhanced remineralization of tooth enamel," *J. Dent. Res.* **89**(11), 1187–1197 (2010).
49. R. S. Jones and D. Fried, "Remineralization of enamel caries can decrease optical reflectivity," *J. Dent. Res.* **85**(9), 804–808 (2006).
50. J. Voronets, T. Jaeggi, W. Buergin, and A. Lussi, "Controlled toothbrush abrasion of softened human enamel," *Caries Res.* **42**, 286–290 (2008).

Downloaded From: http://biomedicaloptics.spiedigitallibrary.org/ on 01/14/2014 Terms of Use: http://spiedl.org/terms

51. T. Jaeggi and A. Lussi, "Toothbrush abrasion of erosively altered enamel after intraoral exposure to saliva: an in situ study," *Caries Res.* **33**, 455–461 (1999).
52. A. Joiner, E. Weader, and T. F. Cox, "The measurement of enamel wear of two toothpastes," *Oral Health Prev. Dent.* **2**(4), 383–388 (2004).
53. A. Joiner, A. Schwarz, C. J. Philpotts, T. F. Cox, K. Huber, and M. Hannig, "The protective nature of pellicle towards toothpaste abrasion on enamel and dentine," *J. Dent.* **36**, 360–368 (2008).
54. J. D. B. Featherstone and A. Lussi, "Understanding the chemistry of dental erosion," in *Dental Erosion from Diagnosis to Therapy*, A. Lussi, Ed., pp. 66–76, Karger AG, Basel (2006).
55. L. Wang, R. Tang, T. Boustein, C. A. Orme, P. J. Bush, and G. H. Nancollas, "A new model for nanoscale enamel dissolution," *J. Phys. Chem. B* **109**, 999–1005 (2005).
56. J. A. Gray, "Kinetics of the dissolution of human dental enamel in acid," *J. Dent. Res.* **41**(3), 633–645 (1962).
57. C. Hannig, D. Berndt, W. Hoth-Hannig, and M. Hannig, "The effect of acidic beverages on the ultrastructure of the acquired pellicle-An *in situ* study," *Arch. Oral Biol.* **54**(6), 518–526 (2009).
58. A. Lussi, T. Jaeggi, and D. Zero, "The role of diet in the aetiology of dental erosion," *Caries Res.* **38**, 34–44 (2004).
59. M. J. Larsen and R. Nyvad, "Enamel erosion by some soft drinks and orange juices relative to their pH, buffering effect and contents of calcium phosphate," *Caries Res.* **33**, 81–87 (1999).
60. A. Lussi, N. Schlueter, E. Rakhmatullina, and C. Ganss, "Dental erosion—an overview with emphasis on chemical and histopathological aspects," *Caries Res.* **45**, 2–12 (2011).
61. A.-K. Johansson, P. Lingström, T. Imfeld, and D. Birkhed, "Influence of drinking method on tooth-surface pH in relation to dental erosion," *Eur. J. Oral Sci.* **112**, 484–489 (2004).
62. S. Al-Khateeb, R. A. M. Exterkate, E. De Josselin de Jong, B. Angmar-Mansson, and J. M. Ten Cate, "Light-induced fluorescence studies on dehydration of incipient enamel lesions," *Caries Res.* **36**, 25–30 (2002).
63. A. Hellen, A. Mandelis, Y. Finer, and B. T. Amaechi, "Quantitative evaluation of the kinetics of human enamel simulated caries using photothermal radiometry and modulated luminescence," *J. Biomed. Opt.* **16**, 071406 (2011).
64. M. E. Barbour and G. D. Rees, "The role of erosion, abrasion and attrition in tooth wear," *J. Clin. Dent.* **17**(4), 88–93 (2006).
65. M. Addy and R. P. Shellis, "Interaction between attrition, abrasion and erosion in tooth wear," *Monogr. Oral Sci.* **20**, 17–31 (2006).

Downloaded From: http://biomedicaloptics.spiedigitallibrary.org/ on 01/14/2014 Terms of Use: http://spiedl.org/terms